Journal of Superconductivity and Novel Magnetism (2021) 34:1133–1139
https://doi.org/10.1007/s10948-021-05823-z

ORIGINAL PAPER

A Theoretical Investigation on the Physical Properties of $SrPd_2Sb_2$ Superconductor

Md. Zahidur Rahaman [1] · M. A. Islam [2]

Received: 3 October 2020 / Accepted: 28 January 2021 / Published online: 24 February 2021

Abstract

The high temperature phase of $SrPd_2Sb_2$ polymorphs exhibits bulk superconductivity below 0.6 K. The electron phonon coupling constant and density of states are two major factors that control the superconductivity in this intermetallic compound. Here we report the detailed physical properties including structural, elastic, electronic, and optical properties of this superconducting phase by using DFT-based computational method. The calculated lattice parameters and density of states show good agreement with the experimental data. This intermetallic is ductile and comparatively soft with respect to other members of this family. This compound exhibits metallic conductivity mostly emerging from Pd and Sb atoms that is different from other similar type of superconducting materials. The strong covalent interactions in Sb-Sb and Sb-Pd bonds define the electronic characteristics of this superconducting material. The optical properties of this superconductor are fairly comparable with other similar compounds in this family.

Keywords Superconductivity · DFT study · Physical properties

1 Introduction

$ThCr_2Si_2$ structured superconductors possess interesting physical properties, e.g., mixed valency, heavy fermion nature, valence fluctuation, etc. These superconducting materials exhibit very rich physics owing to their close energies regarding the charge, spin, and orbital dynamics [1, 2]. The group of ternary intermetallic materials contain more than 2000 representatives [3]. These materials are mostly derived from the $BaAl_4$ type structures. Among these representatives, $ThCr_2Si_2$ structure was first reported by Sikirica et al. in 1965 [4]. A comprehensive geometric investigation of nearly 600 materials in this group had been done by Just et al. in 1996 [5]. In recent years, again $ThCr_2Si_2$-type superconductors have received excessive consideration through the discovery of $(Ba_{0.6}K_{0.4})Fe_2As_2$ high-temperature superconductor with $ThCr_2Si_2$-type structure [6]. In addition, Pd, Pt, and Ni-based $ThCr_2Si_2$-type borocarbides [7–9] have been reported over the last years with relatively high transition temperature. It shows the hope to form a family of novel high temperature superconductors.

Among Pd-based superconductors, the high-temperature phase of $SrPd_2Sb_2$ polymorphs is a familiar low-temperature BCS superconductor with superconducting critical temperature of nearly 0.60 K [10]. This superconducting material possess $ThCr_2Si_2$-type structure with bulk superconductivity. The density of states at Fermi level and electron-phonon coupling are two major factors that determines the transition temperature of this superconductor. It is still interesting to investigate the detailed physical properties of this material for gaining a deep understanding about the structure-property relationship of this material.

Although experimental study on the superconducting properties of $SrPd_2Sb_2$ was done by Kase et al. in 2016 [10], there is no information available in the literature about the detailed physical properties of this material. In this literature, we aim to study the detailed physical properties, e.g., structural, mechanical, electronic, and optical properties of this ternary pnictide $SrPd_2Sb_2$ superconductor. The density functional theory-based theoretical investigation reveals interesting physical properties of this material.

✉ Md. Zahidur Rahaman
md_zahidur.rahaman@unsw.edu.au; zahidur.physics@gmail.com

[1] School of Materials Science and Engineering, Faculty of Science, University of New South Wales, Sydney 2052, Australia

[2] Department of Physics, University of Barisal, Barisal 8200, Bangladesh

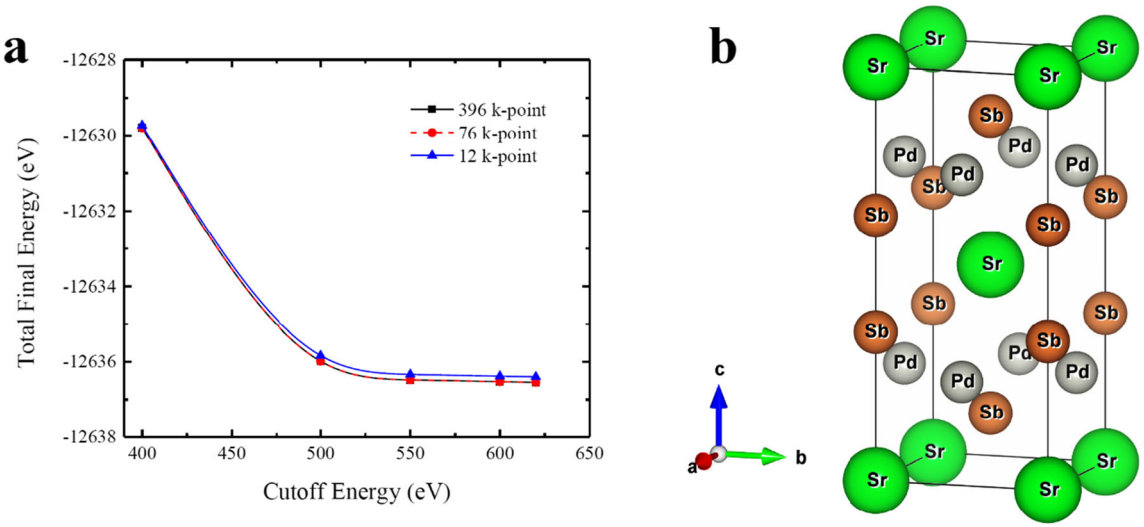

Fig. 1 **a** K-point and planewave cutoff energy convergence result for structure optimization. **b** Crystal structure of the high-temperature phase of $ThCr_2Si_2$-type $SrPd_2Sb_2$ superconductor

2 Theoretical Methodology

The calculations were performed by using the density functional theory-based CASTEP code [11, 12]. Generalized gradient approximation (GGA) with the Perdew-Burke-Ernzerhof (PBE) exchange correlation functional was used for treating the exchange correlation energy [13, 14]. The Pd-$4s^2$ $4p^6$ $4d^{10}$ $5s^{0.5}$, Sb-$4d^{10}$ $5s^2$ $5p^3$, and Sr-$4s^2$ $4p^6$ $5s^2$ were taken as valence electrons for pseudoatomic calculations. The sets of OTFG ultrasoft pseudopotentials with Koelling-Harmon relativistic treatment were employed for calculating the investigated properties of the compound. The Monkhorst-Pack scheme was used to construct the K-point sampling of the Brillouin zone [15]. The wave functions were expanded at 550 eV cut-off energy with 6 × 6 × 8 grids in the primitive cell of $SrPd_2Sb_2$ superconductor. The cut-off energy and K-point are chosen very carefully to obtain the ground state of $SrPd_2Sb_2$ superconductor as shown in Fig. 1a. All the calculations were performed by using the same cut-off energy and K-point to ensure the ground state properties of this superconductor. BFGS (Broyden-Fletcher-Goldfarb-Shanno) relaxation scheme was used for relaxing the crystal structure [16]. The finite strain theory was employed to calculate the elastic stiffness constants of the compound [17]. Volume conserving strains were used in the primitive cell of the reported superconductor. Voigt-Reuss-Hill (VRH) averaging scheme [18] was used for calculating the polycrystalline mechanical parameters from the estimated C_{ij}. The polycrystalline elastic moduli, Pugh's ratio, Poisson's ratio, universal elastic anisotropy, and Vickers hardness were evaluated by using Eqs. (2)-(13) given elsewhere [19]. The optical properties were investigated by using the CASTEP tool based on the standard DFT Kohn-Sham orbitals.

Table 1 Unit cell parameters of $ThCr_2Si_2$-type $SrPd_2Sb_2$ superconductor

Properties	$SrPd_2Sb_2$	
	This study	Expt. [10]
a_0 (Å)	4.692	4.621
c_0 (Å)	11.096	10.776
c_0/a_0	2.364	-
V_0 (Å^3)	244.27	-

3 Results and Discussion

3.1 Structural Properties

The high-temperature phase of $SrPd_2Sb_2$ superconductor belong to the tetragonal crystallographic system with space group *I4/mmm* (139). The conventional unit cell contains ten atoms with two formula units. The optimized crystal structure of $SrPd_2Sb_2$ superconductor is illustrated in Fig. 1b. The calculated and experimental unit cell parameters are tabulated in Table 1. It is evident that the calculated values agree well with the experimental results. This is a good indication about the reliability of the present DFT-based first-principles calculations.

Table 2 The evaluated elastic constants C_{ij} (in GPa) of $SrPd_2Sb_2$ superconductor

Compounds	C_{11}	C_{12}	C_{13}	C_{33}	C_{44}	C_{66}
$SrPd_2Sb_2$	127.45	15.10	49.54	99.78	29.13	11.09
$SrPd_2Ge_2$ [20]	141.05	31.76	65.50	105.79	39.29	21.37

Table 3 Calculated polycrystalline bulk modulus B (GPa), shear modulus G (GPa), Young's modulus E (GPa), B/G values, Poisson's ratio ν, elastic anisotropy A^{U}, and Vickers hardness H_v (GPa) of $SrPd_2Sb_2$ superconductor

Polycrystalline elastic properties							
Compound	B	G	E	B/G	ν	A^{U}	H_v
$SrPd_2Sb_2$	64.74	26.40	69.72	2.45	0.32	1.53	1.75
$SrPd_2Ge_2$ [20]	79.26	32.65	86.12	2.42	0.32	0.78	2.44

3.2 Mechanical Properties

Since the high-temperature phase of the studied superconductor $SrPd_2Sb_2$ belongs to the tetragonal family, it has six independent single crystal elastic constants. The evaluated elastic constants are tabulated in Table 2 with comparison of $SrPd_2Ge_2$ superconductor [20]. It is evident from Table 2 that the calculated elastic constants of $SrPd_2Sb_2$ superconductor are nearly comparable with the $SrPd_2Ge_2$ superconductor as both belong to the same crystal family and share same crystal structure with slightly different chemical compositions. For being mechanically stable in nature a compound with tetragonal structural symmetry should maintain the following stability criteria proposed by Born-Huang [21].

$$\left.\begin{array}{c} C_{11} > 0, C_{44} > 0, C_{33} > 0, C_{66} > 0 \\ C_{11} + C_{33} - 2C_{13} > 0, C_{11} - C_{12} > 0 \\ 2(C_{11} + C_{12}) + C_{33} + 4C_{13} > 0 \end{array}\right\} \quad (1)$$

As shown in Table 2, the calculated elastic constants follow all of the Born-Huang stability criteria implying the mechanical stability of $SrPd_2Sb_2$ superconductor. From Table 2, it is also evident that $C_{11} > C_{33}$. This implies that the atomic bonding between (100) and (001) planes does not have the same strength. The incompressibility along [100] direction is stronger than [001] direction. Again C_{44} is somewhat larger than C_{66} indicating that the [100](001) shear is tougher than the [100](010) shear for this intermetallic.

The polycrystalline mechanical properties are calculated from the single crystal elastic constant values as shown in Table 3. It is evident that the value of bulk modulus, shear modulus, and Young's modulus of $SrPd_2Sb_2$ superconductor are somewhat smaller than those of $SrPd_2Ge_2$ superconductor. It implies that the studied intermetallic is somewhat softer compared with $SrPd_2Ge_2$ superconductor. However, both the superconductors possess smaller elastic moduli compared

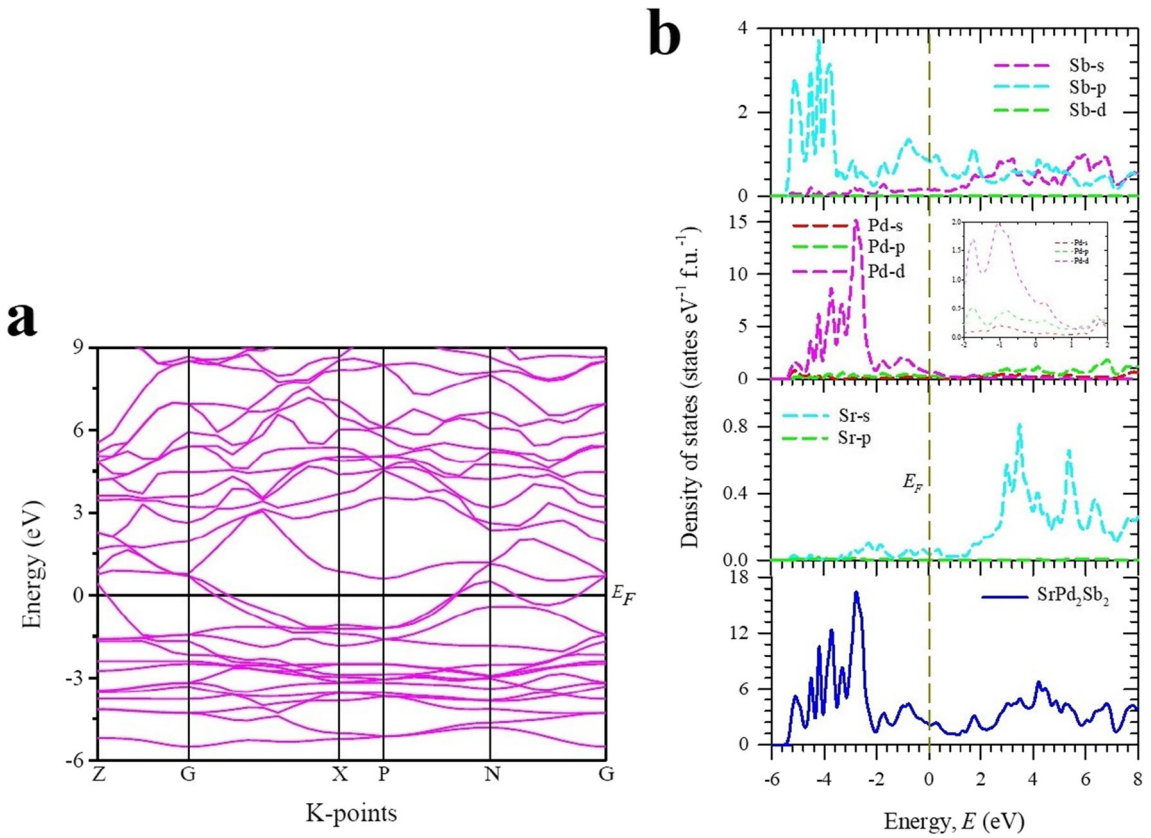

Fig. 2 Electronic band structure **a** and density of states; **b** of $SrPd_2Sb_2$ superconductor

Table 4 Mulliken atomic populations of $SrPd_2Sb_2$ superconductor

	Species	s	p	d	Total	Charge	Bond	Population	Length (Å)
	Sr	2.15	5.98	0.82	8.95	1.05	Pd-Sb	−1.91	2.6862
$SrPd_2Sb_2$	Pd	2.73	6.97	9.40	19.11	−1.11	Sb-Sb	−2.16	2.9326
	Sb	1.21	3.21	10.0	14.42	0.58			

to other members of this family [19, 22] indicating softer nature of these intermetallics.

The Pugh's ratio (B/G) is used to predict the brittleness and ductility of material [23]. $B/G < 1.75$ determines the brittleness of a material otherwise the compound should be ductile. As shown in Table 3, the high-temperature phase of $SrPd_2Sb_2$ is ductile in nature similar as $SrPd_2Ge_2$ superconductor. The Poisson's ratio helps to understand the nature of bonding force in crystal [24]. As shown in Table 3, both the intermetallics possess central force as both of them follow $0.25 < \nu < 0.50$ criteria. The Poisson's ratio is also useful to predict the failure mode of a compound [25, 26]. $\nu < 0.26$ determines the brittleness of a material; otherwise, the compound should be ductile. According to the Poisson's ratio, both the intermetallics are ductile in nature similar as predicted by the Pugh's ratio. The universal elastic anisotropy index A^U is used to estimate the anisotropic nature of a crystal [27]. $A^U = 0$ for a completely isotropic materials otherwise the compound should be anisotropic. From Table 3, it is evident that the studied compound is anisotropic as the value of A^U deviates from zero. The Vickers hardness H_v [28] of a material can be estimated by using a new theoretical model suggested by Chen et al. [29]. The value of H_v is comparatively smaller implying the soft nature of the studied compound similar as predicted by the value of bulk, shear, and Young's modulus.

3.3 Electronic Properties

Figure 2 shows the electronic band structure and density of states (DOS) of $SrPd_2Sb_2$ superconductor. As illustrated in Fig. 2a, there is no band gap at the Fermi level (E_F) as valance band and conduction band overlap with each other. It implies metallic nature of $SrPd_2Sb_2$ superconductor. This electronic behavior is consistent with other similar type of superconducting materials [19, 20, 22, 30]. The partial and total DOS of the studied compound is plotted in Fig. 2b. The valance band is mostly composed of Pd-d and Sb-p states with minor contributions from Sr-s and Sb-s states. On the other hand, the conduction band is mostly composed of Sr-s, Sb-s and Sb-p states. However, Pd-d and Sb-p orbitals contribute most at the Fermi level. Therefore, the metallic conductivity of $SrPd_2Sb_2$ superconductor mostly emerges from Pd and Sb atoms that is different from other similar type of superconducting materials [19, 22]. The calculated DOS at Fermi level $N(E_F)$ is 2.17 states eV^{-1} fu^{-1} that is slightly higher than the experimentally evaluated $N(E_F)$ 1.54 states eV^{-1} fu^{-1} [10]. More experimental and theoretical investigations are required to understand the existing discrepancy between these values.

For gaining comprehensive understanding of the chemical bonding of $SrPd_2Sb_2$, superconductor Mulliken atomic populations [31] have been calculated and analyzed (Table 4). It is evident from Table 4 that Pd atom retains negative charges, whereas Sr and Sb atom retains positive charges. Therefore, charge transfer occurs from Sr and Sb atom to Pd atom [19, 32]. A low value of the bond population specifies the ionic character (for a perfectly ionic interaction, the value of the bond population should be zero), whereas a value deviating1 from zero indicates increasing level of covalency [33]. According to this statement, both the Pd-Sb and Sb-Sb bonds have covalent character. There is no bonding with Sr atoms.

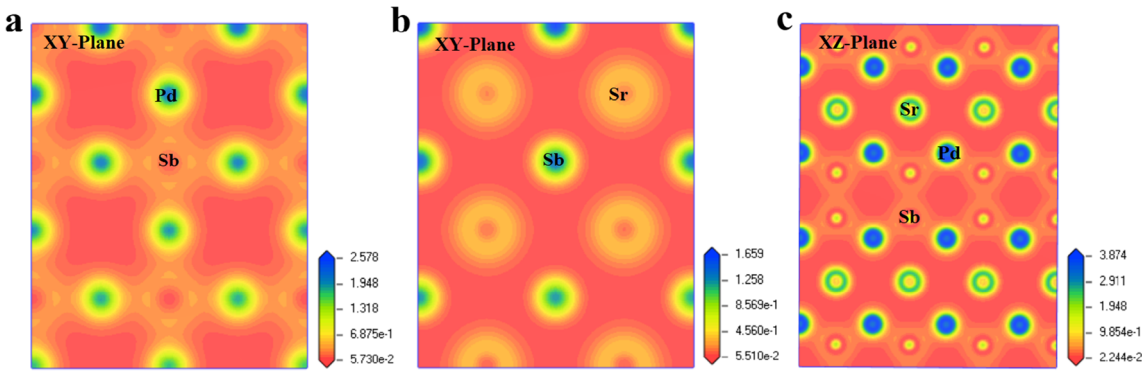

Fig. 3 Charge density map of $SrPd_2Sb_2$ superconductor. **a** Electron distribution of Pd and Sb atoms on XY-plane. **b** Electron distribution of Sb and Sr atoms on XY-plane. **c** Electron distribution of Sr, Pd, and Sb atoms on XZ-plane

The bond length of Pd-Sb and Sb-Sb bonds is also tabulated in Table 4.

For further justification of the above explanation about the chemical bonding of $SrPd_2Sb_2$ superconductor, the total electron density has been calculated. It should be noted that this calculation has been performed by using the conventional unit cell of $SrPd_2Sb_2$ superconductor. Figure 3 exhibits the electron density distribution map of $SrPd_2Sb_2$ superconductor. As shown in Fig. 3a, the charge density of Sb and Pd atoms are overlapped with each other. This implies the covalent character of Pd-Sb bonds [34, 35]. It is clear from Fig. 3b that there is no interaction between Sr and Sb atoms. Figure 3c represents the complete picture of chemical bonding in $SrPd_2Sb_2$ superconductor. Charge sharing between two Sb atoms and Sb and Pd atoms undoubtedly indicates the formation of Sb-Sb and Sb-Pd bonds with covalent character. There is no bonding

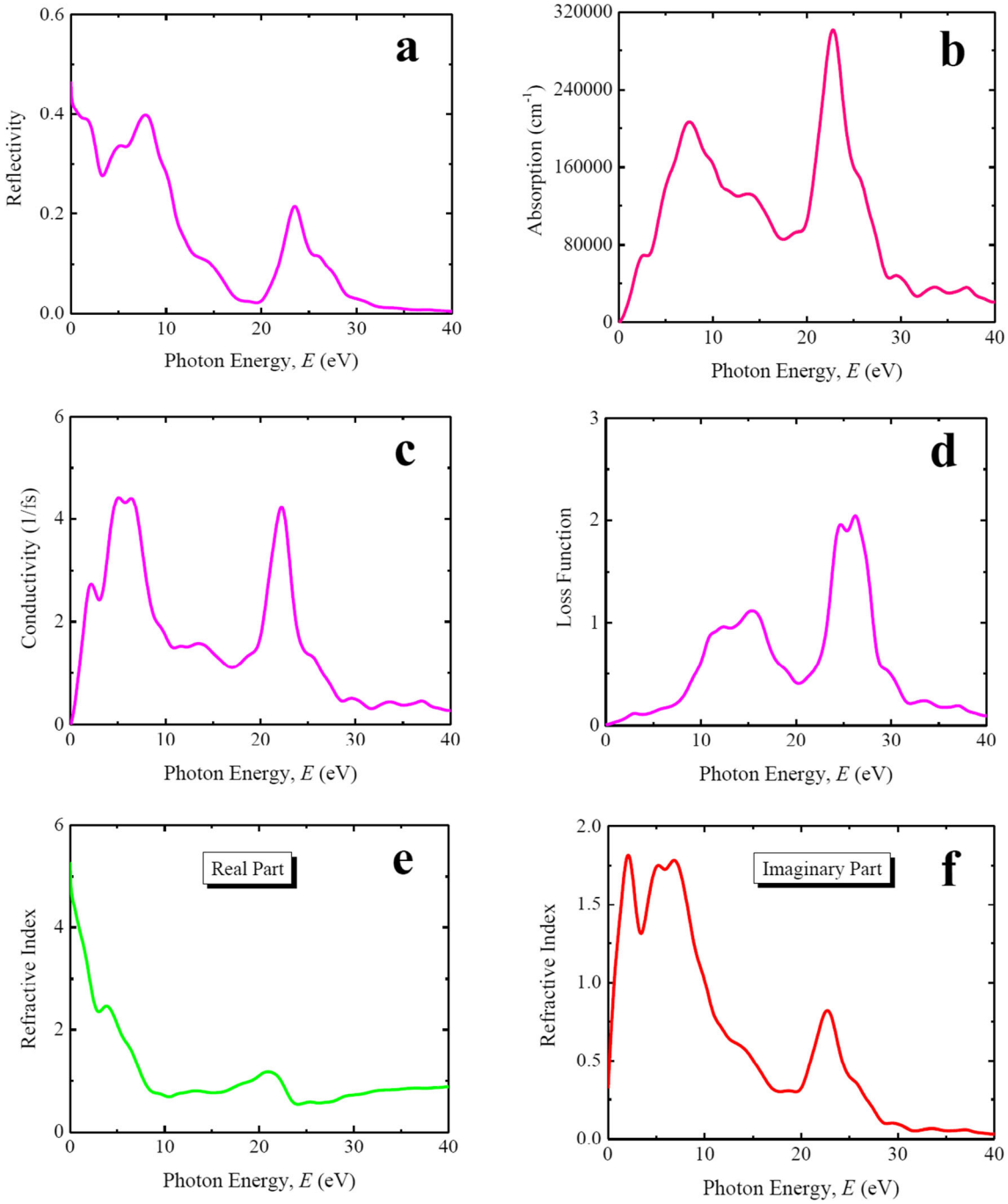

Fig. 4 The optical functions **a** reflectivity, **b** absorption coefficient, **c** conductivity, **d** loss function, **e** real part of refractive index, and **f** imaginary part of refractive index of $SrPd_2Sb_2$ superconductor for polarization vector [100]

with Sr atoms. These strong covalent interactions in Sb-Sb and Sb-Pd bonds define the electronic characteristics of this superconducting material.

3.4 Optical Properties

Optical properties of materials are particularly useful to know the response of a material upon incident electromagnetic wave. For optoelectronic applications, the visible part of electromagnetic spectrum plays a vital role in tuning the efficiency of the respective devices. In this case, the response of a material to visible spectra is crucial. This response can be measured by various optical functions such as, absorption coefficient, reflectivity, optical conductivity, loss function, and refractive index.

The calculated reflectivity of $SrPd_2Sb_2$ superconductor is illustrated in Fig. 4a. The reflectivity of this compound is gradually decreased with the increase in photon energy. The rate of decrement is not linear. Some peaks are observed in the reflectivity spectra. In the infrared and visible region of electromagnetic spectrum, reflectivity is high. It falls sharply in the ultraviolet zone and becomes almost zero after 35 eV (plasma edge) with a sharp peak at 24 eV. Reflectivity of this superconductor is fairly comparable with other similar compounds in this family [20, 36].

The absorption coefficient is defined as the fraction of energy absorbed per unit length of a material [37, 38]. Figure 4b illustrates the absorption spectrum of $SrPd_2Sb_2$ superconductor as a function of incident photon energy up to 40 eV. The absorption spectrum starts from 0 eV, i.e., there is no band gap in $SrPd_2Sb_2$. This finite absorption at low energies indicates the availability of free charge carriers in $SrPd_2Sb_2$, again confirming the metallic nature of this intermetallic as stated in section 3.3 (Fig. 2a). It can also be noted that this compound shows fairly good absorbance at the ultraviolet region with some minima and maxima.

Photon energy dependent optical conductivity of $SrPd_2Sb_2$ superconductor is shown in Fig. 4c. The optical conductivity is finite at 0 eV that again implies the metallic nature of this intermetallic. The optical conductivity increases sharply at the infrared region then starts to decrease at the visible region. The conductivity gradually decreases to zero at the ultraviolet region with some minor peaks. This is a common characteristic of the metallic compounds.

Figure 4d illustrates the energy loss spectrum of $SrPd_2Sb_2$ superconductor as a function of incident photon energy. The loss function indicates the energy loss of a fast electron traversing the material and is large at the plasma frequency [39–42]. Two notable peaks are observed with the prominent one at 26 eV, that corresponds to the rapid drop in the reflectance.

The refractive index of a material is a dimensionless number that describes how fast light travels through the material [43, 44]. The refractive index varies with wavelength. Figure 4e illustrates the real part of refractive index of $SrPd_2Sb_2$ superconductor. The refractive index of this intermetallic is high in the low energy region (infrared region) and gradually falls off in the high energy region (from visible to ultraviolet region). The refractive index of $SrPd_2Sb_2$ superconductor at 2.12 eV (584.83 nm) is 2.933 that is comparatively larger than diamond (2.42 at 589 nm). For a real refractive index, only scattering can occur while for a complex index, both scattering and absorption can take place. The imaginary part of the refractive index is directly responsible for the absorption of the light in the medium. Figure 4f illustrates the imaginary part of refractive index of $SrPd_2Sb_2$ superconductor. The value of the imaginary part of refractive index is low in the infrared region and high in the visible region following the gradual decrease in ultraviolet region.

4 Conclusions

In conclusion, we report the detailed physical properties of a weak-coupling bulk superconductor $SrPd_2Sb_2$ having superconducting critical temperature of 0.6 K. The electron phonon coupling constant and density of states are two major factors that control the superconductivity in this intermetallic compound. This intermetallic is mechanically stable, ductile, and soft in nature. This compound exhibits metallic conductivity emerges from Pd and Sb atoms. The strong covalent interactions in Sb-Sb and Sb-Pd bonds define the electronic characteristics of this superconducting material. This intermetallic shows good reflectivity in the infrared and visible region of electromagnetic spectrum with strong absorbance in the ultraviolet region. This computational aspect will help to understand the basic physical properties of this superconducting polymorph that could be beneficial for future exploration to achieve desired properties in this class of superconductor.

Declarations

Conflict of Interest The authors declare that they have no conflict of interest.

References

1. Stewart, G.: Non-Fermi-liquid behavior in d-and f-electron metals. Rev. Mod. Phys. **73**(4), 797 (2001)
2. Imada, M., Fujimori, A., Tokura, Y.: Metal-insulator transitions. Rev. Mod. Phys. **70**(4), 1039 (1998)
3. Cenzual, Karin. Pearson's crystal data®: crystal structure database for inorganic compounds. Ed. Pierre Villars. Materials Park, OH: ASM International (2007)

4. Ban, Z., Sikirica, M.: The crystal structure of ternary silicides ThM_2Si_2 (M= Cr, Mn, Fe, Co, Ni and Cu). Acta Crystallogr. **18**(4), 594–599 (1965)
5. Just, G., Paufler, P.: On the coordination of $ThCr_2Si_2$ (BaAl4-type compounds within the field of free parameters. J. Alloys Compd. **232**(1-2), 1-25 (1996)
6. Rotter, M., Tegel, M., Johrendt, D.: Superconductivity at 38 K in the iron arsenide $(Ba_{1-x}K_x)Fe_2As_2$. Phys. Rev. Lett. **101**(10), 107006 (2008)
7. Nagarajan, R., et al.: Superconductivity and magnetism in quaternary F (F·Y or f elements) transition metal borocarbides and magnetic properties of RNi_4B (R·Y or rare earth). J. Alloys Compd. **225**(1-2), 571–577 (1995)
8. Cava, R., et al.: Superconductivity in RPt_2B_2C. Phys. Rev. B. **49**(17), 12384 (1994)
9. Cava, R., et al.: Superconductivity in the quaternary intermetallic compounds $LnNi_2B_2C$. Nature. **367**(6460), 252–253 (1994)
10. Kase, N., et al.: Superconductivity in ternary pnictide SrPd2Sb2 Polymorphs. J. Phys. Soc. Jpn. **85**(4), 043701 (2016)
11. Clark, S.J., et al.: First principles methods using CASTEP. Z. Kristallogr. Cryst. Mater. **220**(5-6), 567–570 (2005)
12. Segall, M., et al.: First-principles simulation: ideas, illustrations and the CASTEP code. J. Phys. Condens. Matter. **14**(11), 2717 (2002)
13. Grimme, S.: Semiempirical GGA-type density functional constructed with a long-range dispersion correction. J. Comput. Chem. **27**(15), 1787–1799 (2006)
14. Perdew, J.P., Burke, K., Ernzerhof, M.: Generalized gradient approximation made simple. Phys. Rev. Lett. **77**(18), 3865 (1996)
15. Monkhorst, H.J., Pack, J.D.: Special points for Brillouin-zone integrations. Phys. Rev. B. **13**(12), 5188 (1976)
16. Fischer, T.H., Almlof, J.: General methods for geometry and wave function optimization. J. Phys. Chem. **96**(24), 9768–9774 (1992)
17. Haddow, J., Hrudey, T.: A finite strain theory for elastic-plastic deformation. Int. J. Nonlin. Mech. **6**(4), 435–450 (1971)
18. Hill, R.: The elastic behaviour of a crystalline aggregate. Proc. Phys. Soc., A. **65**(5), 349 (1952)
19. Rahaman, M.Z., Rahman, M.A.: $ThCr_2Si_2$-type Ru-based superconductors $LaRu_2M_2$ (M= P and As): an ab-initio investigation. J. Alloys Compd. **695**, 2827–2834 (2017)
20. Ali, M.S., Rahman, M.A., Rahaman, M.Z.: A theoretical investigation of $ThCr_2Si_2$-type Pd-based superconductors XPd_2Ge_2 (X= Ca, Sr, La, Nd). Physica. C. Supercond. and its Applications. **561**, 35–44 (2019)
21. Born, Max., Kun, Huang.: Dynamical theory of crystal lattices. Clarendon press (1954)
22. Rahaman, M.Z., Rahman, M.A.: Novel 122-type Ir-based superconductors $BaIr_2Mi_2$ (Mi= P and As): a density functional study. J. Alloys Compd. **711**, 327–334 (2017)
23. Pugh, S.: XCII. Relations between the elastic moduli and the plastic properties of polycrystalline pure metals. London, Edinburgh Dublin Philos. Mag. J. Sci. **45**(367), 823–843 (1954)
24. Anderson, O.L., Demarest Jr., H.H.: Elastic constants of the central force model for cubic structures: polycrystalline aggregates and instabilities. J. Geophys. Res. **76**(5), 1349–1369 (1971)
25. Rahaman, M.Z., Ali, M.L., Rahman, M.A.: Pressure-dependent mechanical and thermodynamic properties of newly discovered cubic Na_2He. Chin. J. Phys. **56**(1), 231–237 (2018)
26. Rahaman, M.Z., Ali, M.L.: Insight into the physical properties of two niobium based compounds, Nb_3Be and Nb_3Be_2, via a first principles calculation. Chin. J. Phys. **56**(4), 1386–1393 (2018)
27. Ranganathan, S.I., Ostoja-Starzewski, M.: Universal elastic anisotropy index. Phys. Rev. Lett. **101**(5), 055504 (2008)
28. Smith, R.L., Sandly, G.: An accurate method of determining the hardness of metals, with particular reference to those of a high degree of hardness. Proc. Inst. Mech. Eng. **102**(1), 623–641 (1922)
29. Chen, X.-Q., et al.: Modeling hardness of polycrystalline materials and bulk metallic glasses. Intermetallics. **19**(9), 1275–1281 (2011)
30. Rahman, M.A., et al.: The physical properties of $ThCr_2Si_2$-type nickel-based superconductors $BaNi_2T_2$ (T= P, As): an ab-initio study. Chin. J. Phys. **59**, 58–69 (2019)
31. Mulliken, R.: Electronic population analysis on LCAO-MO molecular wave functions. IJ Chem. Phys. **23**, 1833–1840 (1955)
32. Rahaman, M.Z., Rahman, M.A.: Novel Laves phase superconductor $NbBe_2$: a theoretical investigation. Comput. Condens. Matter. **8**, 7–13 (2016)
33. Segall, M., et al.: Population analysis of plane-wave electronic structure calculations of bulk materials. Phys. Rev. B. **54**(23), 16317 (1996)
34. Rahaman, M.Z., Rahman, M.A., Sarker, M.A.R.: Prediction of a new transition metal oxide $MgRhO_3$ with $SrTiO_3$-type structure: stability, structure and physical characteristics. Chin. J. Phys. **55**(4), 1489–1494 (2017)
35. Kholil, M.I., Rahaman, M.Z., Rahman, M.A.: First principles study of the structural, elastic, electronic, optical and thermodynamic properties of $SrRh_2$ laves phase intermetallic compound. Comput. Condens. Matter. **13**, 65–71 (2017)
36. Parvin, F., Naqib, S.: Structural, elastic, electronic, thermodynamic, and optical properties of layered $BaPd_2As_2$ pnictide superconductor: a first principles investigation. J. Alloys Compd. **780**, 452–460 (2019)
37. Rahaman, M.Z., Hossain, A.M.A.: Effect of metal doping on the visible light absorption, electronic structure and mechanical properties of non-toxic metal halide CsGeCl 3. RSC Adv. **8**(58), 33010–33018 (2018)
38. Ali, M.L., Rahaman, M.Z.: Investigation of different physical aspects such as structural, mechanical, optical properties and Debye temperature of Fe_2ScM (M= P and As) semiconductors: a DFT-based first principles study. International Journal of Modern Physics B. **32**(10), 1850121 (2018)
39. Rahman, M.A., Rahaman, M.Z., Rahman, M.A.: The structural, elastic, electronic and optical properties of MgCu under pressure: a first-principles study. Int. J. Mod. Phys. B. **30**(27), 1650199 (2016)
40. Rahman, M.A., et al.: Theoretical investigation on MgV_2O_6: ab-initio study. Philos. Mag. **98**(22), 2077–2093 (2018)
41. Rahman, M.A., et al.: First principles investigation of structural, electronic and optical properties of NiV2O6. Comput. Condens. Matter. **15**, 95–99 (2018)
42. Ali, M.L., Rahaman, M.Z., Rahman, M.A.: The structural, elastic and optical properties of ScM (M= Rh, Cu, Ag, Hg) intermetallic compounds under pressure by ab initio simulations. Int. J. Comput. Mater. Sci. Eng. **5**(04), 1650024 (2016)
43. Rahman, M.A., Rahaman, M.Z., Sarker, M.A.R.: First principles investigation of structural, elastic, electronic and optical properties of $HgGeB_2$ (BP, As) chalcopyrite semiconductors. Comput. Condens. Matter. **9**, 19–26 (2016)
44. Rahaman, M.Z., Rahman, M.A.: Investigation of the physical properties of two Laves phase compounds HRh_2 (H= Ca and La): a DFT study. Int. J. Mod. Phys. B. **32**(12), 1850149 (2018)